

Superfluid density of ^4He confined in nanopores

K. Yamashita and D. S. Hirashima

Department of Physics, Nagoya University, Nagoya 464-8602, Japan

(Received 4 November 2008; revised manuscript received 5 December 2008; published 5 January 2009)

Helicity modulus in one-dimensional (1D) and anisotropic two-dimensional (2D) classical XY models is calculated. In finite-size 1D lattice, it is unity at absolute zero and rapidly vanishes as temperature increases due to proliferating phase slippage. Similarly, in anisotropic 2D lattice with large aspect ratio, helicity modulus in the direction of the longer side diminishes at a temperature much smaller than Kosterlitz-Thouless transition temperature T_{KT} . This finding is in contrast to the recent observation of finite superfluid density below T_{KT} in ^4He films adsorbed on 1D nanopores. We argue that the superfluid density observed in the experiment is not affected by phase slippage and that is the reason why finite superfluid density was observed. Furthermore, we discuss the observability of genuine 1D behavior of superfluid density in 1D nanopores.

DOI: [10.1103/PhysRevB.79.014501](https://doi.org/10.1103/PhysRevB.79.014501)

PACS number(s): 67.25.dr, 67.25.de, 67.25.dg

I. INTRODUCTION

Bulk liquid ^4He exhibits a second-order phase transition into a superfluid state at the critical temperature $T=T_\lambda=2.18$ K. The transition is accompanied by a sharp peak in specific heat at $T=T_\lambda$. The nature of the phase transition in lower dimensions depends upon the dimensionality of the system. In two dimensions (2D), superfluid long-range order is destroyed by thermal fluctuations at finite temperatures.^{1,2} However, finite superfluid density ρ_s at finite temperatures was observed in ^4He films with a torsional oscillator.³ This behavior was successfully explained with the Kosterlitz-Thouless (KT) theory.⁴⁻⁸ Below the KT transition temperature T_{KT} , the system has quasi-long-range order and finite ρ_s . In one dimension (1D), no long-range order exists either at finite temperatures, but no experimental study had been made so far on strictly 1D liquid ^4He .

Recently, Ikegami *et al.*⁹ and Toda *et al.*¹⁰ succeeded in studying superfluid behavior of ^4He films adsorbed on surfaces of nanopores using a torsional oscillator. Toda *et al.*¹⁰ observed a superfluid transition similar to the bulk one in a ^4He film adsorbed in nanopores that are three-dimensionally interconnected. The superfluid density ρ_s continuously becomes finite below the temperature T_c where a peak in specific heat is observed.¹⁰ They also studied ^4He films adsorbed in 1D nanopores.^{9,10} The pores consist of straight and long channels (the average length is 300 nm). The diameter of pores a is systematically controlled and they studied cases with $a=1.5-4.7$ nm.^{9,10} Adsorbed ^4He atoms can migrate from one channel to another only through edges. The effect of the migration must be very limited, and one can regard the nanopores as almost independent quasi-1D pores. They observed a weak peak in specific heat at $T=T_c$, but no sign of superfluid was found just below T_c . What is puzzling is that they observed a rapid change in the frequency of the torsional oscillator at $T_s(\ll T_c)$. This finding implies finite ρ_s at finite temperatures in 1D, which seems difficult to reconcile with the conventional wisdom that there is no phase transition at a finite temperature in 1D.^{1,2}

Moreover, the onset temperature T_s was found to be close to T_{KT} , which can be estimated by areal density of ^4He at

oms. The questions are then (1) why they were able to observe finite superfluid density in (quasi-)1D ^4He systems at finite temperatures and (2) why the onset temperature is close to T_{KT} , which is a quantity relevant in 2D.

In this study, we argue that the observed superfluid behavior can be naturally explained once the precise meaning of the superfluid density measured with a torsional oscillator is clarified. To do so, we first make it clear how (or why) superfluid density vanishes at a finite temperature in 1D. This is very helpful to understand the behavior of superfluid density in quasi-1D (or anisotropic 2D). Moreover, we discuss observability of the truly 1D superfluid density.

The length ℓ of the pores used in the experiments is around 300 nm, $\ell \approx 300$ nm. It is ^4He atoms in the second layer that form a liquid state, since the ^4He atoms in the first layer form a solid phase and make no contributions to superfluidity.¹⁰ Thus, the diameter of the pores is effectively reduced approximately by 1 nm. Therefore, when the diameter of pores is 2.8 nm,¹⁰ the effective circumference is around 6 nm. We are thus dealing with anisotropic 2D (or quasi-1D) systems of size $\ell_x \times \ell_y$ with $A=\ell_x/\ell_y \approx 50$. In the limit of $A \rightarrow \infty$, the energy necessary for global phase slippage to occur vanishes and it completely destroys superfluid density at a finite temperature. At a finite A , the energy for phase slippage remains finite and superfluid density can also remain finite at temperatures much lower than T_{KT} . However, we argue that the superfluid density observed in a torsional oscillator experiment is not affected by phase slippage and that is why it can remain finite at a finite temperature (comparable to T_{KT}) as has been observed in the experiments.

The superfluid behavior in liquid ^4He can be well studied using a ferromagnetic XY model.¹¹ In Sec. II, we first study 1D and anisotropic 2D (quasi-1D) classical XY models to clarify the characteristic behavior of superfluid density in those systems. In Sec. III, we discuss the experimental results in the light of the results obtained in Sec. II and discuss the possibility of observation of genuine 1D behavior of superfluid density. Section IV is devoted to summary. In the Appendix, we discuss the case with nanopores filled with ^4He liquid.

II. ONE-DIMENSIONAL AND QUASI-ONE-DIMENSIONAL XY MODELS

We first map the ^4He system onto a spin system. It is well known that a hardcore boson system can be mapped onto a ferromagnetic XY model.¹¹ In the mapping, we have to specify the lattice constant d and exchange interaction J . It is natural to assume that the lattice constant is comparable to (or slightly larger than) the average particle-particle distance in the boson system. Exchange interaction can then be estimated by $J \approx \hbar^2 n/m$ (Ref. 11), where n is areal number density and m is the mass of a ^4He atom. Actually, we need not specify the precise value of d because the value of d is not necessarily relevant in studying the behavior of ρ_s as will be shown later.¹² In the following, we put $d=1$ unless otherwise stated.

First we study the 1D classical XY model

$$\mathcal{H} = -J \sum_i \cos(\theta'_{i+1} - \theta'_i), \quad (1)$$

where exchange interactions only between the nearest-neighbor pairs are considered. The total number of lattice points is $N=L_x$. Although the relevance of classical approximation in 1D may be questionable, we study this model because it is instructive for anisotropic 2D cases.

We are concerned in this paper with helicity modulus \bar{Y} .^{13,14} For a uniform twist of the phase θ'_i , $\theta'_i \rightarrow \theta'_i + \Phi_i$ with $\Phi_i = kx_i$, the free-energy density increases as $f(k) = f(0) + \Delta f(k)$. Helicity modulus \bar{Y} is defined as $\Delta f(k) = \frac{1}{2} \bar{Y} k^2$ and has dimension $[\bar{Y}] = E/L^{d-2}$ in d dimensions. Conventionally, it is related to superfluid density through $\bar{Y} = (\frac{\hbar}{m})^2 \rho_s^{\text{H.M.}}$. Here, we put suffix H.M. for later convenience (see Sec. III). In 1D, we obtain¹⁵

$$\frac{\bar{Y}^{(1)}}{J} = Y^{(1)} = E^{(1)} + S^{(1)}, \quad (2)$$

where

$$E^{(1)} = \frac{1}{L_x} \left\langle \sum_i \cos(\theta'_{i+1} - \theta'_i) \right\rangle \quad (3)$$

and

$$S^{(1)} = -\frac{K}{L_x} \left\langle \left[\sum_i \sin(\theta'_{i+1} - \theta'_i) \right]^2 \right\rangle, \quad (4)$$

where $K = \beta J = J/(k_B T)$.

In 1D, ρ_s must vanish at finite temperatures in the limit of $L_x \rightarrow \infty$, but it remains finite for a finite L_x . Now we study ρ_s in 1D for a finite L_x . In considering the 1D chain, it is essential to take account of the possibility of global phase slippage. We rewrite the phase variable θ'_i as $\theta'_i = \theta_i + (2\pi n_x i)/L_x$. The phase variable θ_i satisfies $\theta_i = \theta_{i+L_x}$ if the periodic boundary condition is imposed. Then, the Hamiltonian is rewritten as

$$\mathcal{H} = -J \sum_i [\cos \nu_x \cos \delta\theta_i - \sin \nu_x \sin \delta\theta_i], \quad (5)$$

where $\delta\theta_i = \theta_{i+1} - \theta_i$, $\nu_x = 2\pi n_x/L_x$, and the partition function $Z^{(1)}$ can be written as $Z^{(1)} \approx Z_s^{(1)} \langle e^I \rangle_s$, where $Z_s^{(1)} = Z_{\text{ps}}^{(1)} Z_p^{(1)}$,

$$Z_{\text{ps}}^{(1)} = \sum_{n_x=-\infty}^{\infty} e^{-(K/2)L_x \nu_x^2}, \quad (6)$$

$$Z_p^{(1)} = \int \prod_{\ell} \frac{d\theta_{\ell}}{2\pi} \exp\left(K \sum_i \cos \delta\theta_i \right), \quad (7)$$

$$I = \frac{K}{2} \nu_x^2 \left[L_x - \sum_i \cos \delta\theta_i \right] - K \nu_x \sum_i \sin \delta\theta_i, \quad (8)$$

and $\langle \cdots \rangle_{\lambda}$ stands for the average with $Z_{\lambda}^{(1)}$. Phase slippage contributes to $Z_{\text{ps}}^{(1)}$, but does not to $Z_p^{(1)}$. Since, from Eq. (6), it is clear that $\langle n_x^2 \rangle \propto L_x/K$, we have safely neglected terms of higher orders of ν_x . In the limit $L_x/K \rightarrow \infty$, the phase slippage occurs freely, leading to vanishing $Y^{(1)}$. However, at $K \gtrsim L_x$, which is possible for finite L_x , $Y^{(1)}$ can remain finite.

At low temperatures, $K \gg 1$, we can carry out spin-wave expansion and obtain $Z_p^{(1)} \approx Z_{\text{sw}}^{(1)} \langle e^Q \rangle_{\text{sw}} \approx Z_{\text{sw}}^{(1)} e^{\langle Q \rangle_{\text{sw}}}$, where

$$Z_{\text{sw}}^{(1)} = e^{KL_x} \int \prod_{\ell} \frac{d\theta_{\ell}}{2\pi} \exp\left(-\frac{K}{2} \sum_i \delta\theta_i^2 \right), \quad (9)$$

$\langle Q \rangle_{\text{sw}} = K \sum_i \langle \delta\theta_i^4 \rangle_{\text{sw}} / 24 = L_x / (8K)$. We then obtain $\ln Z^{(1)} \approx \ln Z_s^{(1)} \approx \ln Z_{\text{sw}}^{(1)} + \langle Q \rangle_{\text{sw}} + \mathcal{O}(1)$. As $\ln Z_s^{(1)}$ and I are quantities of $\mathcal{O}(1)$, they make only negligible contributions to $\ln Z^{(1)}$, but they have to be taken account of when calculating averages with $Z_s^{(1)}$.

Now, we calculate helicity modulus $Y^{(1)}$ in the 1D XY model. The first term $E^{(1)}$ is readily calculated as

$$E^{(1)} = \frac{1}{L_x} \frac{\partial \ln Z^{(1)}}{\partial K} \approx 1 - \frac{1}{2K} - \frac{1}{8K^2}. \quad (10)$$

Note that the phase slippage makes no contribution to $E^{(1)}$. For $S^{(1)}$, after a straightforward calculation, we obtain

$$S^{(1)} = -Ks(1) + \left[s(1) - \frac{K}{4}s(2) + \frac{K}{4}s(1)^2 \right] + \Delta S^{(1)}, \quad (11)$$

where

$$\Delta S^{(1)} = -\frac{2s(1)^2 + 2Ks(1)^3 - 3Ks(1)s(2)}{32} - \frac{8/K - 16s(1) - 2Ks(2) + K^2s(3)}{32K}, \quad (12)$$

and

$$s(k) = \left\langle \left[\frac{(2\pi n_x)^2}{L_x} \right]^k \right\rangle_{\text{ps}}. \quad (13)$$

Here, we have used the identities $\sum_i \delta\theta_i = 0$, $\langle \sum_i \delta\theta_i^2 \rangle_s \approx L[1/K + 1/(2K^2)]$, $\langle [\sum_i \delta\theta_i^3]^2 \rangle_s \approx 9L/K^3$.

At $K \gg L_x$, $s(k)$ vanishes exponentially, $s(k) \approx 2[(2\pi)^2/L_x]^k e^{-2\pi^2 K/L_x}$, i.e., no phase slippage occurs, and

$S^{(1)} \simeq -1/(4K^2)$. Thus, helicity modulus $Y^{(1)}$ is given by

$$Y^{(1)} \simeq 1 - \frac{1}{2K} - \frac{3}{8K^2}, \quad (14)$$

at $K \gg L_x$. On the other hand, at $K \ll L_x$, $s(k) = (2k-1)!!/K^k + \delta s(k)$, where $\delta s(k) \propto (L_x/K)^k e^{-L_x/(2K)}/K$. Then, at $1 \ll K \ll L_x$, we obtain $S^{(1)} = -1 + 1/(2K) + 1/(8K^2) + \delta S^{(1)} = -E^{(1)} + \delta S^{(1)}$, where $\delta S^{(1)}$ is exponentially small. We finally have

$$Y^{(1)} = \delta S^{(1)} \simeq e^{-L_x/(2K)} \ll 1 \quad (15)$$

at $1 \ll K \ll L_x$. In the limit of $L_x \rightarrow \infty$, Y_x vanishes at any finite K due to phase slippage. This is in perfect harmony with the conventional wisdom.

The results obtained so far can be easily understood by studying the correlation function $C(i-j)$ defined by

$$C(i-j) = \langle \cos(\theta'_i - \theta'_j) \rangle = \left\langle \cos \frac{2\pi n_x(i-j)}{L_x} \right\rangle_{\text{ps}} \langle \cos(\theta_i - \theta_j) \rangle_p. \quad (16)$$

It is easily shown that

$$\begin{aligned} & \left\langle \cos \frac{2\pi n_x(i-j)}{L_x} \right\rangle_{\text{ps}} \\ &= \begin{cases} 1 - \left[1 - \cos \frac{2\pi(i-j)}{L_x} \right] e^{-2\pi^2 K/L_x}, & K \gg L_x \\ \exp \left[-\frac{1}{2} \frac{L_x}{K} \left(\frac{i-j}{L_x} \right)^2 \right], & 1 \ll K \ll L_x \end{cases} \end{aligned} \quad (17)$$

and that

$$\langle \cos(\theta_i - \theta_j) \rangle_p \simeq \exp \left[-\frac{L_x}{2K} \frac{|i-j|}{L_x} \right], \quad K \gg 1. \quad (18)$$

We can see that $C(i-j) \sim 1$ at $K \gg L_x$ and decays exponentially as $|i-j| \rightarrow \infty$ at $K \ll L_x$. Phase slippage is not necessary for the absence of long-range order in 1D. Usually, it is Eq. (18) that leads to absence of long-range order in 1D. However, for the destruction of helicity modulus, phase slippage [Eq. (17)] plays a role.

The above analyses are confirmed by Monte Carlo (MC) calculations. In the MC simulations, we used the Wolff cluster algorithm.¹⁶ We typically carried out $(1-4) \times 10^6$ measurements after $(2-3) \times 10^4$ thermalization steps. The periodic boundary condition is imposed. Specific heat has a weak peak at $T \simeq 0.4J$ (Fig. 1); the position and the height are insensitive to L_x . At $L_x = 48$, $Y^{(1)}$ rapidly increases from zero at $T \simeq 0.2J$ and merges to a straight line, $E^{(1)} \simeq 1 - 1/(2K)$, at $T \simeq 0.05J$. When L_x increases $Y^{(1)}$ and $S^{(1)}$ shift to lower temperatures, while $E^{(1)}$ hardly shifts. These results are in good agreement with the spin-wave analysis.

Now we move on to anisotropic 2D cases. In anisotropic 2D systems, we can define helicity modulus \bar{Y}_x along the x direction and \bar{Y}_y along the y direction. They are explicitly given by

$$\bar{Y}_\mu = Y_\mu = E_\mu + S_\mu, \quad \mu = x, y, \quad (19)$$

where

$$E_\mu = \frac{1}{L_x L_y} \left\langle \sum_i \cos(\theta'_{i+\mu} - \theta'_i) \right\rangle, \quad (20)$$

and

$$S_\mu = -\frac{K}{L_x L_y} \left\langle \left[\sum_i \sin(\theta'_{i+\mu} - \theta'_i) \right]^2 \right\rangle, \quad (21)$$

where μ is a unit vector along the μ direction.

We rewrite the partition function Z by taking explicit account of the phase slippage. The phase slippage term Z_{ps} for the 2D XY model is given by

$$Z_{\text{ps}} = \sum_{n_x, n_y = -\infty}^{\infty} e^{-(K/2)[(2\pi n_x)^2/A + A(2\pi n_y)^2]}, \quad (22)$$

where $A = L_x/L_y$. When $A \geq 1$, the phase slippage along the y direction is severely restricted as long as $K \geq 1/A$.¹⁷ Therefore, in a quasi-1D case, i.e., at $A \gg 1$, we can safely put $n_y = 0$, that is, neglect the possibility of phase slippage along the y direction. Then, the problem is reduced to the same one as the 1D XY model except for the replacement of length L_x with the ratio A . There is, however, a crucial difference from the 1D case. In 1D, finite $Y^{(1)}$ at finite temperatures is obtained only for a finite-size lattice, but, in 2D, finite helicity modulus Y_x at a finite temperature can be realized in the limit of $L_x, L_y \rightarrow \infty$ for a finite A .

At low temperatures $K \gg 1$, the spin-wave expansion is valid, and repeating the same calculations, we obtain

$$E_x \simeq 1 - \frac{1}{4K} - \frac{1}{8K^2} \quad (23)$$

and

$$S_x \simeq -Ks(1) + \frac{1}{2} \left[s(1) - \frac{Ks(2)}{4} + \frac{Ks(1)^2}{4} \right] + \Delta S_x, \quad (24)$$

where

$$\begin{aligned} \Delta S_x &= -\frac{2s(1)^2 + 2Ks(1)^3 - 3Ks(1)s(2)}{128} \\ &\quad - \frac{4/K - 16s(1) - 2Ks(2) + K^2s(3)}{128K}. \end{aligned} \quad (25)$$

At $K \gg A$, $s(\nu)$ is exponentially small and $\Delta S_x \simeq -1/(32K^2)$. Then, we have

$$Y_x \simeq 1 - \frac{1}{4K} - \frac{5}{32K^2}. \quad (26)$$

On the other hand, at $1 \ll K \ll A$,

$$Y_x \simeq e^{-A/(2K)} \ll 1. \quad (27)$$

In the same way as in 1D, Y_x remains finite at $K \gg A$ because the global phase slippage is prohibited, but vanishes at $K \ll A$ due to the proliferating phase slippage. In quasi-1D, A

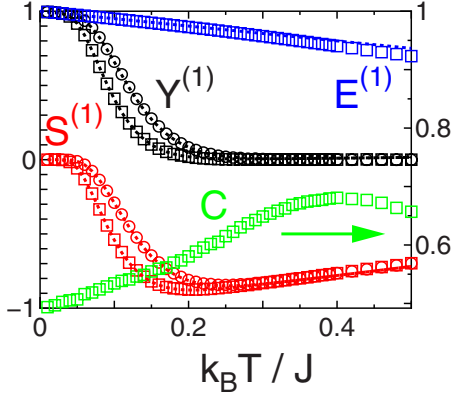


FIG. 1. (Color online) Helicity modulus $Y^{(1)}=E^{(1)}+S^{(1)}$ in the 1D XY model of length $L_x=48$ (dots) and 64 (squares). Dotted curves are the results of spin-wave expansion discussed in the text. Specific heat per spin is also shown. Error bars are smaller than the size of symbols.

$\gg 1$, the phase rigidity is completely destroyed by phase slippage before nonlinear excitations such as vortices make a contribution.

Figure 2 shows specific heat C and helicity moduli, Y_x and Y_y , in the 2D XY models. In the isotropic case, $A=1$, specific heat takes a maximum at $T=T_c \approx 1.05J$, and the helicity modulus has a (universal) jump at $T=T_{KT} \approx 0.9J$.¹⁸ At $A=1$, $Y_x=Y_y$. This means that J/k_B roughly corresponds to the KT transition temperature T_{KT} of a 2D ⁴He film of the same density. When A deviates from unity, the peak in specific heat is reduced, but its position is almost unchanged at $T=T_c \approx 1.05J$. Helicity modulus Y_y slightly increases at $T > T_{KT}$, but Y_x along the x axis rapidly shifts to low temperatures. However, at the low-temperature limit, $K \gg A$, Y_x merges to Y_y and reaches unity at $T=0$. As is shown in Fig. 2(b), for a fixed value of L_y , specific heat C and helicity modulus Y_y are independent of L_x , but Y_x shifts to low temperatures as L_x increases (as A increases). On the other hand, for a fixed value of A , helicity modulus Y_x falls onto a common curve for different values of L_x and L_y , but specific heat C and Y_y depend on L_x and L_y as is shown in Fig. 2(c). These results for Y_x are well explained by the spin-wave analysis. In two dimensions, the spin-wave part (the second factor) of the correlation function, Eq. (16), obeys the power law (in the spin-wave expansion). It is clear that the softening of the helicity modulus solely originates from the phase slippage contribution.

III. COMPARISON WITH THE EXPERIMENTS

Now we discuss the experimental findings in the light of the results obtained so far. The onset temperature T_s of finite superfluid density found by Ikegami *et al.*⁹ and Toda *et al.*¹⁰ roughly corresponds to the KT transition temperature $T_{KT} = (\pi/2)(\hbar/m)^2 \rho_s(T_{KT})/k_B \approx (\pi/2)(\hbar/m)^2 \rho/k_B$. This is in marked contrast to our finding: the onset temperature of Y_x in anisotropic 2D ($A \gg 1$) is much reduced from T_{KT} . We then have to clarify what is really measured or calculated.

This question has actually been discussed by several authors.^{19–21} Helicity modulus Y stands for the rigidity of a

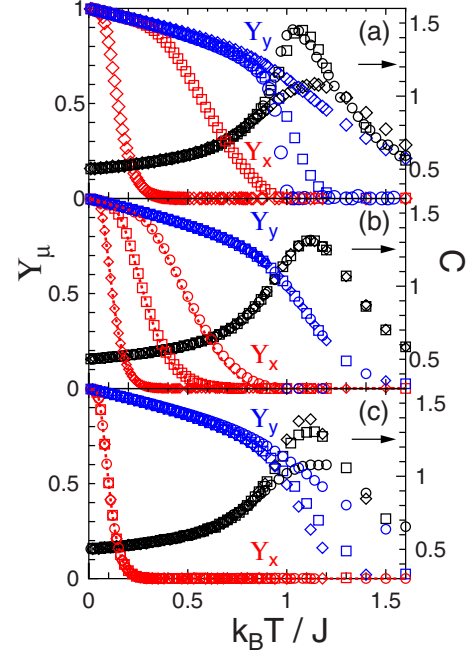


FIG. 2. (Color online) Helicity moduli, Y_x and Y_y , and specific heat C in the 2D XY model. (a) Lattice size is $160 \times L_y$; $L_y = 160(A=1)$ (dots), $20(A=8)$ (squares), and $4(A=40)$ (diamonds). (b) Lattice size is $L_x \times 8$; $L_x = 80(A=10)$ (dots), $160(A=20)$ (squares), and $400(A=50)$ (diamonds). (c) Ratio $A=L_x/L_y$ is fixed, $A=60$; $L_x=240$ (dots), 480 (squares), and 720 (diamonds). Error bars are smaller than the size of symbols. Dotted curves represent results of the spin-wave analysis.

system against infinitesimal phase *difference* between both ends of the system and includes contributions from phase slippage as was discussed in Sec. II. Although the phase difference is infinitesimally small, the phase gradient, i.e., the superflow velocity, may not be small. Thus, in calculating helicity modulus, we take account of states with finite superflow velocity. For pores of length $\ell_x=300$ nm, the typical superflow velocity v_s is $v_s \approx \hbar/(m\ell_x) \sim 30$ cm/s, which is much larger than the velocity v_{torsion} induced by a torsional oscillator.²² Typical frequency of a torsional oscillator is 1000 Hz and its typical amplitude is 1 nm. Therefore, $v_{\text{torsion}} \sim 10^{-4}$ cm/s $\ll v_s$.

Helicity modulus \bar{Y} [or the superfluid density $\rho_s^{\text{H.M.}}$ defined by $\rho_s^{\text{H.M.}} = (\hbar/m)^{-2} \bar{Y}$] is thus suitable for study of thermodynamic properties such as thermodynamic phase transition, but it is not necessarily the quantity measured in dynamical measurements such as torsional oscillator experiments. If the frequency is so small that $\omega\tau \ll 1$, then, it is possible to observe $\rho_s^{\text{H.M.}}$, where τ is the relaxation time for the superflow state. In the experiment where $\omega\tau \gg 1$, the response to a given velocity v_{torsion} is measured²⁰ and the measured superfluid density ρ_s is the coefficient in the increase of free-energy density Δf under a fixed superflow velocity, $\Delta f = (1/2)\rho_s v_s^2$. It is difficult to estimate the value of τ , but it is reasonable to assume that $\omega\tau \gg 1$ holds in torsional oscillator experiments.^{19,20} Thus, the superfluid density measured with a torsional oscillator is ρ_s , i.e., the rigidity of a system against infinitesimal phase *gradient* (not phase difference), and is not affected with the phase slippage.

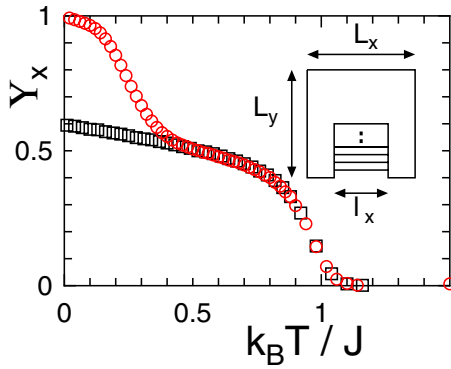


FIG. 3. (Color online) Helicity modulus Y_x in a square lattice $L_x \times L_y$ ($L_x=L_y=40$) part of which is replaced with $n(=19)$ chains of length $\ell_x(=20)$. Open squares stand for Y_x without contribution from the chains.

The above relation is explicitly discussed by Prokof'ev and Svistunov²¹ and Melko *et al.*²³ They derived the relation

$$\rho_s^{\text{H.M.}} = \rho_s \left[1 - \frac{\rho_s}{k_B T} \left\langle \frac{(2\pi n_x)^2}{A} \right\rangle \right] \quad (28)$$

in anisotropic 2D.²⁴ It is clear that $\rho_s^{\text{H.M.}}=0$ does not necessarily mean $\rho_s=0$ and that $\rho_s = \rho_s^{\text{H.M.}}|_{\langle n_x^2 \rangle=0}$. It is not easy to calculate Y_x with the additional constraint $\langle n_x^2 \rangle=0$, but as $A=L_x/L_y$ becomes small, $\langle n_x^2 \rangle \rightarrow 0$ at $K \geq 1$. Therefore,

$$\rho_s \approx \rho_s^{\text{H.M.}}(A \approx 1) \approx \rho_s^{\text{H.M.}} \quad \text{in 2D.} \quad (29)$$

That is why it was observed that $T_s \sim T_{\text{KT}}$ in the experiment,^{9,10} although the frequency shift of a torsional oscillator was caused by 1D ^4He atoms.

It is possible that extrinsic effects such as strong randomness of the substrate may substantially reduce τ and the condition $\omega\tau \ll 1$ may be realized. In this case, the genuine 1D behavior, i.e., the suppression of the onset temperature of superfluidity, would be observed. In the experiments of Ikegami *et al.*⁹ and Toda *et al.*,¹⁰ not only ^4He atoms adsorbed on inner walls of pores, but also ^4He atoms adsorbed on outer walls of grains contribute to superfluid density.^{9,10} It is more realistic to consider the situation where both a 2D film and quasi-1D pores can contribute to superfluid density. In Fig. 3, we show the temperature dependence of Y_x in a square lattice part of which is replaced with chains (see inset). There is no direct interaction between chains. Helicity modulus rises at $T \sim T_{\text{KT}}$, where chains make no contribution to helicity modulus. At $T \approx 0.4J$, the chains also contribute to helicity modulus and Y_x increases rapidly again. This is the behavior of superfluid density that would be observed in an experiment when $\omega\tau \ll 1$ holds. Indeed, quite similar behavior of the frequency shift of a torsional oscillator has been reported so far.²⁵ However, it is premature to draw any conclusion about this.

Thus far, we have considered the case with ^4He films adsorbed on inner walls of nanopores. Now, a preliminary report of an experiment on liquid ^4He filling 1D nanopores has been made.²⁵ To describe this case, an anisotropic three-dimensional (3D) lattice (a bar) $L_x \times L_y \times L_z$ with L_z

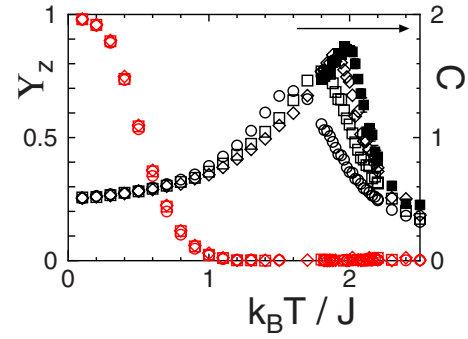


FIG. 4. (Color online) Helicity modulus Y_z and specific heat C in an anisotropic 3D XY model of size $L_x \times L_y \times L_z$. The ratio $B=L_z/L_x^2$ is fixed, $B=10$, and $L_z=160$ (open dots), 360 (open squares), 640 (open diamonds), and 1000 (solid squares). Error bars for Y_z are smaller than the size of symbols.

$\gg L_x, L_y$, is more suitable. In this case, helicity modulus Y_z also becomes soft due to phase slippage, $\langle n_z^2 \rangle \neq 0$, at $1 \ll K \ll B=L_z/(L_x L_y)$. Presumably, it is not $\rho_s^{\text{H.M.}}$, but ρ_s , that is observed with a torsional oscillator in this case, too. However, it is also possible to observe $\rho_s^{\text{H.M.}}$ if the condition $\omega\tau \ll 1$ should be satisfied. Numerical results for classical XY model on anisotropic 3D are given in the Appendix.

IV. SUMMARY

In summary, we have explicitly shown that the helicity modulus in 1D or quasi-1D vanishes at finite temperatures due to proliferating phase slippage and that the onset of superfluid density observed in the experiments of Ikegami *et al.*⁹ and Toda *et al.*¹⁰ experiments can be explained if what they measure is not the helicity modulus, but the rigidity of the system against infinitesimal phase gradient. This clear distinction of the two superfluid densities, $\rho_s^{\text{H.M.}}$ and ρ_s , is unique in (quasi-)1D.²¹ It is highly desired that characteristic behavior of $\rho_s^{\text{H.M.}}$ in (quasi-)1D is observed in experiments and the distinction of the two superfluid densities is really confirmed experimentally.

ACKNOWLEDGMENTS

We thank M. Hieda, T. Matsushita, Y. Minato, T. Minoguchi, S. Miyashita, and N. Wada for useful discussions and comments. This work was partially supported by a Grant-in-Aid for JSPS (Contract No. 165881).

APPENDIX: SUPERFLUID DENSITY IN NANOPORES FULLY FILLED WITH ^4He

For study of superfluid density in a full-pore condition, an anisotropic 3D lattice is appropriate. Here, we consider a classical XY model on a lattice $L_x \times L_y \times L_z$ with $L_z \gg L_x, L_y$. The relevant parameter is the ratio $B=L_z/(L_x L_y) (\gg 1)$. In contrast to the aspect ratio A in 2D cases, parameter B depends on the lattice constant d . If we retain d , parameter B is expressed as $B=\ell_z d/(\ell_x \ell_y) \approx \ell_z d/s$, where ℓ_μ is the length of the system in the μ direction and s is the cross sectional area of a pore. For a pore of length $\ell_z \approx 300$ nm and diameter a

≈ 2 nm, $B \approx 100d$ (nm) ≈ 30 , when $d \approx 0.3$ nm. In the limit of $B \rightarrow \infty$, helicity modulus Y_z vanishes at a finite temperature due to phase slippage, but remains constant at $K \gtrsim B$ for a finite B . In the bulk limit, i.e., in the limit of $L_\mu \rightarrow \infty$ with the ratio $L_x:L_y:L_z$ fixed, B vanishes in proportion to $1/L_\mu$ and no phase slippage occurs.²¹

Figure 4 shows the MC results for specific heat C and helicity modulus Y_z in the XY model of size $L_x \times L_y \times L_z$ for a fixed value of $B(=10)$. In the MC simulation, we use the open boundary condition in the x and y directions and the periodic boundary condition in the z direction. We also use the staggered boundary condition in the x and y directions,^{26,27} which requires vanishing order parameter on the boundary layer, and find that the results are very similar to those obtained with the open boundary condition. Specific heat C has a finite-size effect. Its scaling function was studied in Refs. 26 and 27. In the limit of $L_x, L_z \rightarrow \infty$, C must

diverge at the bulk transition temperature $T_\lambda \approx 2.20J$.²⁸ On the other hand, Y_z falls onto a common curve for different values of L_x and L_z as is expected. In a torsional oscillator experiment using nanopores filled with ^4He , one can measure the superfluid density ρ_s without contributions from phase slippage. One then expects that ρ_s rises at around $T = T_\lambda$ if pores are immersed into bulk liquid ^4He . In their experiments, Taniguchi and Suzuki²⁵ observed rise of superfluid density at $T \approx T_\lambda$ and also observed additional increase (bend) at a lower temperature (~ 0.9 K). Whether this additional increase in ρ_s is related to ^4He liquid in pores remains to be seen. Here, we only mention that the relaxation time τ of ^4He atoms may strongly depend upon the dimensionality of the system and therefore observability of truly 1D behavior may also be different in ^4He films adsorbed on inner walls of pores and in liquid ^4He that fills pores.

¹N. D. Mermin and H. Wagner, Phys. Rev. Lett. **17**, 1133 (1966).

²P. C. Hohenberg, Phys. Rev. **158**, 383 (1967).

³D. J. Bishop and J. D. Reppy, Phys. Rev. Lett. **40**, 1727 (1978).

⁴V. L. Berezinskii, Sov. Phys. JETP **34**, 610 (1972).

⁵J. M. Kosterlitz and D. J. Thouless, J. Phys. C **6**, 1181 (1973).

⁶J. M. Kosterlitz, J. Phys. C **7**, 1046 (1974).

⁷D. R. Nelson and J. M. Kosterlitz, Phys. Rev. Lett. **39**, 1201 (1977).

⁸V. Ambegaokar, B. I. Halperin, D. R. Nelson, and E. D. Siggia, Phys. Rev. B **21**, 1806 (1980).

⁹H. Ikegami, Y. Yamato, T. Okuno, J. Taniguchi, N. Wada, S. Inagaki, and Y. Fukushima, Phys. Rev. B **76**, 144503 (2007).

¹⁰R. Toda, M. Hieda, T. Matsushita, N. Wada, J. Taniguchi, H. Ikegami, S. Inagaki, and Y. Fukushima, Phys. Rev. Lett. **99**, 255301 (2007).

¹¹T. Matsubara and H. Matsuda, Prog. Theor. Phys. **16**, 569 (1956).

¹²Here, we implicitly assume that the particle-particle distance is smaller than the circumference of pores. In the experiment of Toda *et al.*,¹⁰ the average distance is 0.3–0.5 nm.

¹³M. E. Fisher, M. N. Barber, and D. Jasnow, Phys. Rev. A **8**, 1111 (1973).

¹⁴T. Ohta and D. Jasnow, Phys. Rev. B **20**, 139 (1979).

¹⁵S. Teitel and C. Jayaprakash, Phys. Rev. B **27**, 598 (1983).

¹⁶U. Wolff, Phys. Rev. Lett. **62**, 361 (1989).

¹⁷In the isotropic case, $A=1$, no phase slippage is allowed as long as $T \lesssim J$. That is why the possibility of phase slippage is seldom discussed in the 2D XY model. The effect of vortices becomes dominantly important before the global phase slippage makes a significant contribution.

¹⁸For a precise determination of T_{KT} , see M. Hasenbusch, J. Phys. A **38**, 5869 (2005), and references therein.

¹⁹T. Minoguchi and Y. Nagaoka, Prog. Theor. Phys. **80**, 397 (1988).

²⁰J. Machta and R. A. Guyer, J. Low Temp. Phys. **74**, 231 (1989).

²¹N. V. Prokof'ev and B. V. Svistunov, Phys. Rev. B **61**, 11282 (2000).

²² $\langle v_s^2 \rangle = A(\hbar/m\ell_x)^2 s(1) \approx A(\hbar/m\ell_x)^2$ at $K \approx 1$. It is difficult to compare this value with the actual critical velocity in the pore.

²³R. G. Melko, A. W. Sandvik, and D. J. Scalapino, Phys. Rev. B **69**, 014509 (2004).

²⁴From Eqs. (23) and (24), we obtain $\rho_s^{\text{H.M.}} \sim J[1 - \beta J s(1)] + \dots = \rho_s^{\text{bare}}[1 - \beta \rho_s^{\text{bare}} s(1)] + \dots$ at $K \gg 1$.

²⁵J. Taniguchi and M. Suzuki, J. Low Temp. Phys. **150**, 347 (2008).

²⁶N. Schultka and E. Manousakis, Phys. Rev. Lett. **75**, 2710 (1995).

²⁷N. Schultka and E. Manousakis, J. Low Temp. Phys. **111**, 783 (1998).

²⁸W. Janke, Phys. Lett. A **148**, 306 (1990).